Journal of Sound and Vibration 328 (2009) 85–91

Contents lists available at ScienceDirect

Journal of Sound and Vibration

journal homepage: www.elsevier.com/locate/jsvi

Sound generated by vortex ring impingement on a heated wall

E. Giannos Kotsari, M.S. Howe *

Boston University, College of Engineering, 110 Cummington Street, Boston, MA 02215, USA

ARTICLE INFO

Article history:
Received 9 March 2009
Accepted 3 August 2009
Handling Editor: P. Joseph
Available online 25 August 2009

ABSTRACT

An analysis is made of the sound generated when a vortex ring impinges normally on a heated section of a plane wall. The unsteady convective diffusion occurring when the vortex is close to the wall causes a rapid increase in heat transfer and the emission of sound of monopole type. The approximate dependence on vortex Reynolds number of the enhancement of heat transfer is deduced from recent experiments reported by Arévalo et al. [Vortex ring head-on collision with a heated vertical plate, *Physics of Fluids* 19 (2007) 083603-1–083603-9], and is used to derive a scaling law for the acoustic pressure. The sound pressure signature is dominated by a large amplitude pulse associated with an explosive, but brief increase in the rate of heat transfer at the start of the vortex–wall interaction. The quadrupole sound pressure also produced during impingement on the wall is found to be smaller than the thermally induced sound by a factor proportional to $M^2 T_0/(T_w - T_0)$ where M, T_w, T_0 respectively denote the Mach number of the vortex motion, the mean wall temperature and the fluid temperature at large distances from the wall.

1. Introduction

The enhancement of heat transfer between a surface and a flow frequently depends on convective diffusion produced by artificially induced secondary flows in the boundary layer. For example, this can be achieved in a passive manner by the deployment of surface mounted vortex generators. Accomplishments in this area are reviewed by Jacobi and Shah [1] and by Kondjoyan et al. [2]. Heat transfer can also be actively controlled by disrupting the boundary layer by means of small jets, by electrical body forces in the flow, and by acoustic excitation (see e.g. [3–8]).

However, the resulting increases in boundary layer turbulence intensity and fluid heating can produce large increases in the levels of aerodynamically generated sound. Practical problems of this kind are encountered in combustion-driven systems such as gas turbines, rocket motors and furnaces, where unsteady heating is often coupled to acoustic resonances producing structural fatigue and damage [9–11]. Typical flow velocities in such systems are at relatively low Mach number, so that the usual quadrupole excitation of sound by the turbulence Reynolds stress tends to be much weaker than the dipole and monopole sources associated, respectively, with nonuniform acceleration of variable temperature fluid elements and localised volumetric pulsations caused by combustion or unsteady heat transfer from a hot surface [10].

Arévalo et al. [12] investigated vorticity enhanced heat transfer produced by a vortex ring impinging at very low Mach number on a heated wall. They used a simple experimental arrangement that permitted the vortex ring to be generated in a reproducible and carefully controlled manner, independently of the thermal properties of the flow at the wall, and measured the unsteady heat transfer caused by the disruption by the vortex of a nominally steady laminar boundary flow

* Corresponding author.
E-mail address: mshowe@bu.edu (M.S. Howe).

0022-460X/$ - see front matter © 2009 Elsevier Ltd. All rights reserved.
doi:10.1016/j.jsv.2009.08.003

over the heated wall. This flow–surface interaction is far removed from those typically responsible for heat transfer in ducted turbulent flows, but it may be regarded as an elementary model for studying wall cooling in gas turbines by an array of impinging jets. Similarly, there exists an abundance of analytical and experimental results for vortex impact on *unheated* plane walls which can be used to interpret experimental observations [13–16].

This canonical experiment provides sufficient data for the initial theoretical investigation described in this paper of the problem of sound generation by the monopole source produced by the unsteady heat transfer from the wall. In particular, the data given in [12] can be used to deduce the approximate dependence on vortex ring Reynolds number of the maximum increase in the rate of heat transfer. This enables a scaling law to be derived for the amplitude of the peak heat source acoustic pressure in terms of parameters describing the vortex and the heated wall. Time series data of the measured unsteady heat transfer, kindly made available by Dr. R.H. Hernández, permit a detailed picture to be obtained of the acoustic pressure signature, and of its relation to the vortex–wall interaction. For the very low Mach number experiments discussed in [12] it is easily shown that the conventional quadrupole noise produced by the impinging vortex is negligible.

The Arévalo et al. [12] experiment is discussed in Section 2, including the dependence of the maximum heat transfer rate on the vortex ring Reynolds number. The acoustic analogy equation [10] is used in Section 3 to deduce a scaling law for the sound, to derive the acoustic pressure signature, and to compare predictions with the conventional quadrupole sound of the vortex ring interacting with the heated surface.

2. Vortex ring impinging on a heated wall

2.1. The experiment of Arévalo et al. [12]

The experiment performed by Arévalo et al. [12] is illustrated schematically in Fig. 1. A vortex ring is created by the ejection at low Mach number of a slug of air from a circular aperture of diameter D in the vertical, plane wall of a 'vortex ring generator'. The ring travels horizontally by self-induction and impinges at normal incidence on a vertical plate of respective horizontal and vertical dimensions 10×20 cm. The mean translational speed U of the vortex is determined by observation of the travel time over the distance ℓ between the generator and plate. Measurements were made for $D = 13$, 15, 17 mm at Reynolds number $\mathrm{Re} = UD/\nu$ in the range 200–1000, where ν is the kinematic viscosity of the air.

Let coordinate axes $\mathbf{x} = (x, y, z)$ be defined such that the axis of symmetry of the vortex lies along the x-axis, the y-axis is vertical, and the surface of the target plate wetted by the impinging vortex coincides with the plane $x = -0$, so that the vortex approaches the plate from $x < 0$. A square section of the plate centred on the coordinate origin O, with vertical and horizontal sides of length $H = 5.08$ cm, is electrically heated to a steady uniform temperature $T = T_w$ that exceeds the ambient mean temperature T_0. In the absence of the impinging vortex the heated section produces a steady natural convection flow in the adjacent air in $x < 0$. An inertial boundary layer forms at the lower edge of the plate, and a thermal boundary layer (shown in Fig. 2a) starts at the lower edge of the hot square section. The steady rate of heat transfer Q_0, say, across the thermal boundary layer from the plate to the air is given approximately by [17]

$$Q_0 \sim \tfrac{1}{2} G^{1/4} H \rho_0 c_p \chi (T_w - T_0), \tag{1}$$

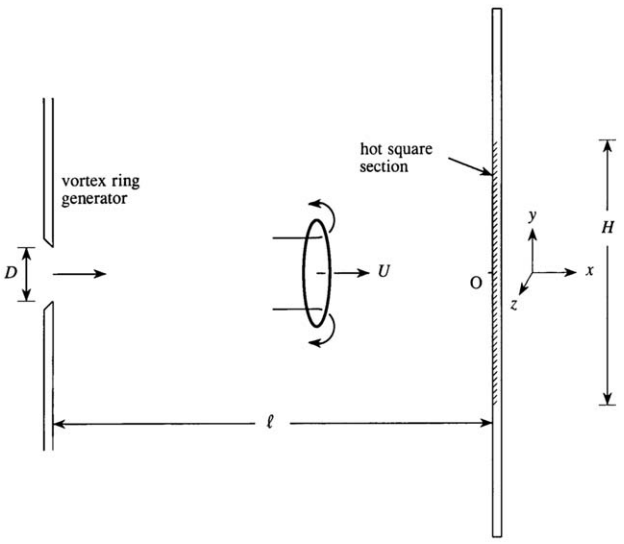

Fig. 1. Schematic of the experiment performed by Arévalo et al. [12].

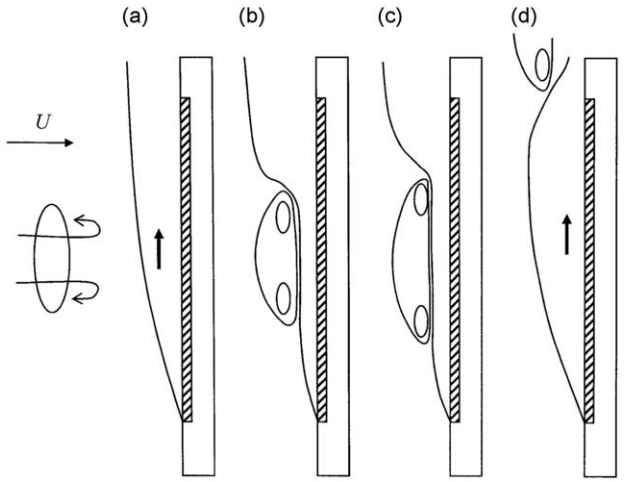

Fig. 2. Illustrating the various stages of the interaction of the vortex ring with the thermal boundary layer (after Arévalo et al. [12]).

where ρ_0, c_p, χ, respectively, denote the mean density, specific heat at constant pressure and the thermal diffusivity of the air, G is the Grashof number

$$\mathrm{G} = \frac{gH^3(T_w - T_0)}{\nu^2 T_0}, \tag{2}$$

and g the acceleration due to gravity. In the experiments $T_0 = 300\,\mathrm{K}$ and $T_w - T_0 = 20\,\mathrm{K}$, so that $\mathrm{G}\sim 4.25\times 10^5$. The boundary layer over the heated section of the plate is therefore laminar [17] and (because the Prandtl number $\mathrm{P} = \nu/\chi \approx 0.73$ for air) the characteristic thickness of both the thermal and inertial boundary layers at the upper end of the heated section is $\delta \sim 2H/\mathrm{G}^{1/4} \sim 0.4\,\mathrm{cm}$, where also the characteristic flow speed U_b in the boundary layer is

$$U_b \sim 0.5\sqrt{\frac{gH(T_w - T_0)}{T_0}} \quad (\sim 10\,\mathrm{cm/s}). \tag{3}$$

This steady state is disrupted by an impinging vortex. Fig. 2 illustrates schematically stages of the interaction of the vortex ring with the buoyancy induced natural convection of the air close to the plate. The vortex begins to influence the flow at the wall when it is within a distance of order D. During an initial time interval $\tau_1 \sim D/U$ the vortex distorts and penetrates the thermal and inertial boundary layers while maintaining its circular ring shape; it exhibits an almost explosive radial expansion over the heated surface and simultaneously produces a significant and rapid increase in the rate of heat transfer (Fig. 2b,c). Shortly after the end of this initial period the vortex diameter is comparable with the size H of the heated section of the plate. The heat transfer rate next begins to decay slowly as both the expanded vortex ring and the boundary layer perturbations are convected upwards and away from the hot section of the plate by the natural buoyancy flow at speed $\sim U_b$ (Fig. 2d).

Arévalo et al. [12] determined the variation with time t of the perturbation $Q'(t)$ in the heat transfer rate produced by the vortex by measuring the changes in the electrical power necessary to maintain the heated section of the plate at temperature T_w. Fig. 3 shows the measured values of $Q'(t)/Q_0$ reported in their paper for the case where $D = 17\,\mathrm{mm}$, $U = 0.55\,\mathrm{m/s}$ ($\mathrm{Re}\sim 650$). The vortex arrives within a distance D of the plate at time $t \approx 0.5\,\mathrm{s}$. There is a rapid increase in $Q'(t)$ over a time $\sim D/U$ up until the ring has expanded to about the size of the heated section of the plate. This is followed by a period of decay of length $\tau_2 \sim H/U_b$ (effectively independent of the Reynolds number Re of the vortex) during which the size of the vortex footprint on the hot region decreases because of the buoyant convection of the vortex away from the heated section of the plate. The subsequent behaviour of the observed heat transfer represents its slow relaxation back to the steady state of natural convection over the heated plate.

2.2. Reynolds number dependence of the excess rate of heat transfer

The peak $Q'_{\max}$ in the *excess* rate of heat transfer $Q'(t)$ produced by an incident vortex occurs shortly after the influence of the wall is first felt by the vortex, during its rapid increase in diameter. Enhanced rates of heat transfer are the result of convective diffusion by the velocity field of the vortex close to the plate. Because diffusivity has the dimensions of velocity × length, the additional convective component of diffusivity must be associated with a characteristic velocity × a suitable 'mixing length' [18]. During the first stages of the interaction, when the vortex approaches within a distance $\sim D$, the 'eddy diffusivity' must therefore be proportional to UD ($\gg \chi$). Comparison with Eq. (1) for the steady heat transfer rate

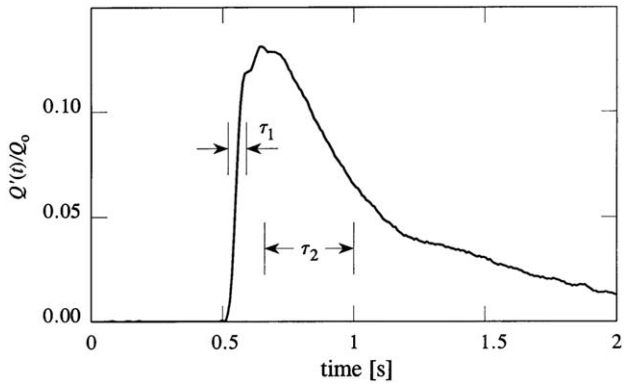

Fig. 3. Unsteady component of the heat transfer rate $Q'(t)/Q_0$ measured by Arévalo et al. [12] when $D = 17\,\text{mm}$, $U = 0.55\,\text{m/s}$, $T_0 = 300\,\text{K}$, $T_w - T_0 = 20\,\text{K}$.

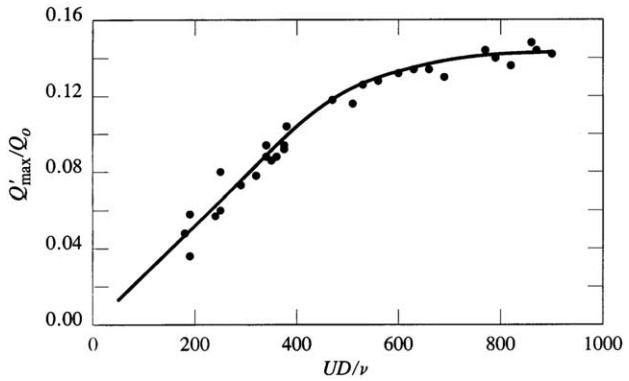

Fig. 4. Dependence on vortex ring Reynolds number UD/ν of the maximum excess rate of heat transfer $Q'_{\max}/Q_0$ when $T_0 = 300\,\text{K}$, $T_w - T_0 = 20\,\text{K}$; • • • measurements of Arévalo et al. [12].

Q_0 accordingly suggests that the maximum excess rate of heat transfer produced by the vortex is given by a relation of the form

$$Q'_{\max} = \frac{\alpha UD}{\chi} Q_0 = \frac{1}{2}\alpha \mathrm{G}^{1/4}\rho_0 c_p UDH(T_w - T_0) \tag{4}$$

for some suitable dimensionless coefficient α. This implies that

$$\frac{Q'_{\max}}{Q_0} = \alpha\,\mathrm{P}\,\mathrm{Re}, \tag{5}$$

where $\mathrm{P} = 0.73$ is the Prandtl number of air.

The series of experiments reported by Arévalo et al. [12] were conducted at fixed values of T_0, T_w. The coefficient α can therefore depend only on the vortex Reynolds number $\mathrm{Re} = UD/\nu$. The data points in Fig. 4 (taken from Fig. 6(a) of [12]) represent the dependence of $Q'_{\max}/Q_0$ on Reynolds number observed in tests performed over a range of values of both D and U. The smooth curve in the figure is our interpolation of these measurements. This indicates that the dimensionless excess heat flux $Q'_{\max}/Q_0$ varies linearly with Reynolds number for $\mathrm{Re} < 600$, and in this range α is constant and given approximately by $\alpha \approx 3.6 \times 10^{-4}$ when $\mathrm{P} = 0.73$. Saturation occurs above $\mathrm{Re} \sim 600$, presumably because larger and/or faster vortex rings are rapidly expanded in size at the plate and spend shorter times over the heated section, reflecting a progressive decrease in the value of α with increasing Reynolds number.

3. The generated sound

At low Mach numbers the production of sound is governed by the aeroacoustic equation [10]

$$\left(\frac{1}{c_0^2}\frac{\partial^2}{\partial t^2} - \nabla^2\right) B = \mathrm{div}(\boldsymbol{\omega} \wedge \mathbf{v} - T\nabla s) + \frac{\partial}{\partial t}\left(\frac{\beta T}{c_p}\frac{\mathrm{D}s}{\mathrm{D}t}\right), \tag{6}$$

where (taking air to be an ideal gas) $B = c_pT + \frac{1}{2}v^2$ is the total enthalpy, s is the specific entropy, β and c_p are, respectively, the coefficient of expansion and specific heat at constant pressure, $\mathbf{v}$ is the velocity and $\boldsymbol{\omega} = \mathrm{curl}\,\mathbf{v}$ is the vorticity. The terms on the right hand side formally represent dipole and monopole sources, respectively. When the Mach number is small the acoustic far field is dominated by the multipole source of lowest order [10] so that, in particular, only the monopole contribution from the entropy s need be retained. The vorticity source actually reduces to a very much weaker source of quadrupole type; it will be retained because it determines the radiation in the absence of heating.

In the acoustic domain the unsteady motion is linear and fluctuations in $B = p/\rho_0$, where p denotes the acoustic perturbation pressure and ρ_0 is the mean air density. To a sufficient approximation we can then write Eq. (6) in the form

$$\left(\frac{1}{c_0^2}\frac{\partial^2}{\partial t^2} - \nabla^2\right)p = \rho_0 \mathrm{div}(\boldsymbol{\omega}\wedge\mathbf{v}) + \frac{\partial}{\partial t}\left(\frac{\rho_0}{c_p}\frac{\mathrm{D}s}{\mathrm{D}t}\right), \tag{7}$$

wherein we have put $\beta = 1/T$ for an ideal gas.

3.1. The thermally induced sound

The quantity $q(\mathbf{x},t) \equiv \rho T \mathrm{D}s/\mathrm{D}t$ is the rate of addition of heat per unit volume of the air. In a first approximation the pressure is uniform across the thermal interaction region, so that $\rho T \approx \rho_0 T_0$ and

$$\frac{\partial}{\partial t}\left(\frac{\rho_0}{c_p}\frac{\mathrm{D}s}{\mathrm{D}t}\right) = \frac{\partial}{\partial t}\left(\frac{\rho_0 q}{c_p \rho T}\right) \approx \frac{\partial}{\partial t}\left(\frac{q}{c_p T_0}\right). \tag{8}$$

The wavelength of the sound is very much larger than the plate when the Mach number of the source flow is infinitesimal. This means that the far field characteristics of the thermal monopole sound are effectively uninfluenced by the presence of the plate [10,19–22]. Therefore, if the sound can propagate freely in all directions from the neighbourhood of the plate, the thermally induced acoustic pressure $p_{\mathrm{Q}}(\mathbf{x},t)$, say, is given in the far field by

$$\begin{aligned} p_{\mathrm{Q}}(\mathbf{x},t) &\approx \frac{1}{4\pi|\mathbf{x}|c_pT_0}\frac{\partial}{\partial t}\int \mathrm{q}\left(\mathbf{y}, t-\frac{|\mathbf{x}|}{c_0}\right)d^3\mathbf{y}, \quad |\mathbf{x}|\to\infty \\ &= \frac{1}{4\pi|\mathbf{x}|c_pT_0}\frac{\partial Q'}{\partial t}\left(t-\frac{|\mathbf{x}|}{c_0}\right). \end{aligned} \tag{9}$$

The order of magnitude of p_{Q} is determined by recalling that the maximum excess heat transfer rate $Q'_{\max}$ is produced over a time $\tau_1 \sim D/U$, so that

$$\frac{\partial Q'}{\partial t} \sim \frac{UQ'_{\max}}{D}. \tag{10}$$

Using this and the approximation (4) in Eq. (9), we find

$$p_{\mathrm{Q}} \sim \rho_0 U^2 \frac{\alpha \mathrm{G}^{1/4}}{8\pi}\frac{H}{|\mathbf{x}|}\left(\frac{T_w - T_0}{T_0}\right). \tag{11}$$

In the particular case illustrated in Fig. 3 that was examined experimentally by Arévalo et al. [12]: $D = 17\,\mathrm{mm}$, $U = 0.55\,\mathrm{m/s}$, $T_0 = 300\,\mathrm{K}$, $T_w - T_0 = 20\,\mathrm{K}$. Then $\mathrm{Re} = UD/\nu \approx 650$, and Eq. (5) and the curve in Fig. 4 supply the value $\alpha \approx 2.8\times 10^{-4}$. Hence Eq. (11) yields the order of magnitude estimate

$$\frac{p_{\mathrm{Q}}}{\rho_0 U^2 (D/|\mathbf{x}|)} \sim 6\times 10^{-5}. \tag{12}$$

The corresponding non-dimensional acoustic pressure signature is determined from Eq. (9) by using the measured time dependence of $Q'(t)/Q_0$ shown in Fig. 3, and by writing

$$\frac{p_{\mathrm{Q}}(\mathbf{x},t)}{\rho_0 U^2 (D/|\mathbf{x}|)} = \frac{\mathrm{G}^{1/4}}{8\pi\,\mathrm{Re}\,\mathrm{P}}\left(\frac{T_w - T_0}{T_0}\right)\frac{H}{U}\frac{\partial}{\partial t}\left[\frac{Q'}{Q_0}\right]_{t-|\mathbf{x}|/c_0}. \tag{13}$$

The predicted wave profile is depicted in Fig. 5, plotted as a function of the retarded time $t - |\mathbf{x}|/c_0$. Evidently the radiation consists principally of an acoustic pulse of magnitude $p_{\mathrm{Q}}/\rho_0 U^2 (D/|\mathbf{x}|) \sim 3\times 10^{-5}$, in good accord with the estimate (12). This pulse is generated during the initial instants of the period of width $\sim\tau_1 = D/U$ in which the vortex first influences the convective boundary layer on the heated section of the plate.

3.2. The quadrupole sound

The 'vortex sound' produced by the impinging vortex is governed by the source $\mathrm{div}(\boldsymbol{\omega}\wedge\mathbf{v})$ of Eq. (6). The generation mechanism can be interpreted as follows: during the initial period of the interaction with the plate the effective source is equivalent to the quadrupole sound p_{quad}, say, produced by the head-on collision of the vortex ring with its 'image' in the plate [23–27]. This sound must be augmented by a very low Reynolds number contribution from vorticity generated on the

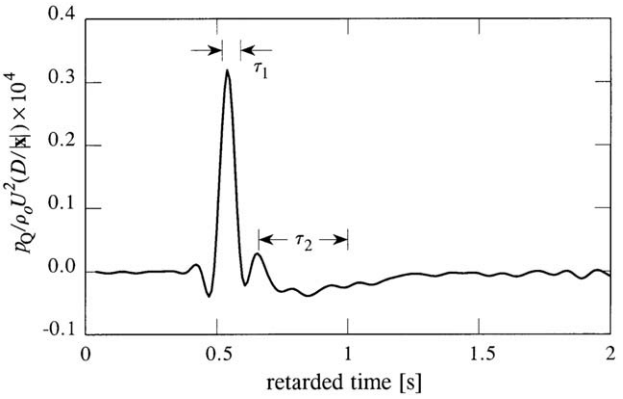

Fig. 5. Monopole acoustic pressure $p_Q(\mathbf{x},t)/\rho_0 U^2(D/|\mathbf{x}|)\times 10^4$ determined by Eq. (13) for $D=17$ mm, $U=0.55$ m/s, $T_0=300$ K, $T_w-T_0=20$ K, plotted as a function of the retarded time $t-|\mathbf{x}|/c_0$.

wetted surface of the plate which, however, is at most of the same order as p_{quad}. The latter can easily be estimated from results given by Kambe and Minota [24], from which we deduce the order of magnitude estimate

$$p_{\text{quad}}\sim A\rho_0 U^2 M^2\,\frac{D}{|\mathbf{x}|},\quad M=\frac{U}{c_0},\quad A\approx 1. \tag{14}$$

Vortex sound is also generated when the remnants of the expanding vortex ring are convected in the buoyant boundary layer flow past the upper edge of the plate. This radiation is nominally of dipole strength and could in principle be stronger than p_{quad}. But it should actually be ignored, because the relevant comparison for applications to hot, turbulent boundary layer flows is between the radiation levels of the thermal and vortex sound during the initial interaction period $\sim O(D/U)$. In that case

$$\frac{p_{\text{quad}}}{p_{\text{Q}}}\sim\frac{8\pi A M^2}{\alpha G^{1/4}}\frac{D}{H}\left(\frac{T_0}{T_w-T_0}\right)\sim 0.04, \tag{15}$$

which indicates that, at least for the parameter ranges of the present experiments, the vortex sound is always small compared to the thermal monopole noise.

4. Conclusion

Unsteady heat addition to a fluid is a source of sound of 'monopole' type. When the ring vortex approaches to within about a diameter D from the heated section of the wall the experimental results reported by Arévalo et al. [12] and others (e.g. Walker et al. [13]) indicate that significant boundary layer distortion occurs close to the wall. This produces a temporary, but 'explosive' increase in the heat transfer rate, of the order of 15% for the Arévalo et al. tests, but occurring sufficiently rapidly that the monopole sound pressure (proportional to the rate of change of the heat transfer rate) is caused to exhibit a large peak. The pressure signature consists of a large pressure pulse entirely dominated by this initial interaction, followed by a relatively weak, oscillatory tail. The subsequent development of the vortex–wall interaction, although it can involve rapid boundary layer growth accompanied by complex and localised boundary layer separation, including the formation of secondary vortex rings at the wall [13–16], is not acoustically important, and contributes relatively little but the weak fluctuating tail to the pressure signature. Similarly, the amplitude of the quadrupole sound produced by the surface interaction is smaller than the monopole radiation by a factor proportional to $M^2T_0/(T_w-T_0)$, where M is the nominal Mach number of the vortex velocity field, although the constant of proportionality may be large.

In a more practical flow regime, involving forced thermal convection over a wall in a mean flow at speed U, fluctuations in the rate of heat transfer between the surface and the flow will vary typically on a time scale $\sim O(\delta/v_*)$, where v_*, δ are, respectively, the boundary layer friction velocity and thickness. Our results suggest that it is reasonable to anticipate that enhanced rates of heat transfer will vary approximately linearly with Reynolds number $v_*\delta/\nu$, a conclusion that is not inconsistent with observation [2], and that it will be accompanied by enhanced levels of boundary layer noise.

Acknowledgements

The authors are grateful to Dr. R.H. Hernández for supplying the experimental data for the plot of Fig. 3. The work of E.G.K. was supported by the award of a Graduate Teaching Fellowship by the Department of Mechanical Engineering of Boston University.

References

[1] A.M. Jacobi, R.K. Shah, Heat transfer surface enhancement through the use of longitudinal vortices: a review of recent progress, *Experimental Thermal and Fluid Science* 11 (1995) 295–309.
[2] A. Kondjoyan, F. Peneau, H.-C. Boisson, Effect of high free stream turbulence on heat transfer between plates and air flows: a review of existing experimental results, *International Journal of Thermal Science* 41 (2002) 1–16.
[3] X. Zhang, Interaction between a turbulent boundary layer and elliptic and rectangular jets, in: W. Rodi, F. Marticelli (Eds.), *Engineering Turbulence Modeling and Experiments*, Vol. 2, Elsevier, New York, 1993, pp. 251–260.
[4] P.R. Voke, S. Gao, Numerical study of heat transfer from an impinging jet, *International Journal of Heat Transfer* 41 (1998) 671–680.
[5] F.A. Kulacki, J.H. Davidson, P.F. Dunn, Convective heat transfer with electric and magnetic field, in: S. Kakac, R.K. Shah, W. Aung (Eds.), *Handbook of Single-Phase Heat Transfer*, Wiley, New York, 1987 (Chapter 9).
[6] M.M. Ohadi, N. Sharaf, D.A. Nelson, Electrohydrodynamic enhancement of heat transfer in a shell-and-tube heat exchanger, *Experiments in Heat Transfer* 4 (1991) 19–39.
[7] R. Lemlich, Vibration and pulsation boost heat transfer, *Chemical Engineering* May (1961) 171–176.
[8] A. Gopinath, A.F. Mills, Convective heat transfer from a sphere due to acoustic streaming, *Journal of Heat Transfer* 115 (1993) 332–341.
[9] N.A. Cumpsty, Jet engine combustion noise: pressure, entropy and vorticity perturbations produced by unsteady combustion or heat addition, *Journal of Sound and Vibration* 66 (1979) 527–544.
[10] M.S. Howe, *Acoustics of Fluid–Structure Interactions*, Cambridge University Press, Cambridge, 1998.
[11] M. Heckl, M.S. Howe, Stability analysis of the Rijke tube with a Green's function approach, *Journal of Sound and Vibration* 305 (2007) 672–688.
[12] G. Arévalo, R.H. Hernández, C. Nicot, F. Plaza, Vortex ring head-on collision with a heated vertical plate, *Physics of Fluids* 19 (2007) 083603-1–083603-9.
[13] J.D.A. Walker, C.R. Smith, A.W. Cerra, T.L. Doligalski, The impact of a vortex ring on a wall, *Journal of Fluid Mechanics* 181 (1987) 99–140.
[14] P. Orlando, R. Verzicco, Vortex rings impinging on walls: axisymmetric and three-dimensional simulations, *Journal of Fluid Mechanics* 256 (1993) 615–646.
[15] C.-C. Chu, C.-T. Wang, C.-C. Chang, A vortex ring impinging on a solid plane surface—vortex structure and surface force, *Physics of Fluids* 7 (1995) 1391–1401.
[16] D. Fabris, D. Liepmann, D. Marcus, Quantitative experimental and numerical investigation of a vortex ring impinging on a wall, *Physics of Fluids* 8 (1996) 2640–2649.
[17] H. Schlichting, *Boundary Layer Theory*, seventh ed, McGraw-Hill, New York, 1979.
[18] J.O. Hinze, *Turbulence*, second ed., McGraw-Hill, New York, 1975.
[19] L. Rayleigh, *Theory of Sound*, Vol. 2, Dover, New York, 1945.
[20] L.D. Landau, E.M. Lifshitz, *Fluid Mechanics*, second ed., Pergamon, Oxford, 1987.
[21] A.D. Pierce, *Acoustics, An Introduction to its Principles and Applications*, American Institute of Physics, New York, 1989.
[22] D.G. Crighton, A.P. Dowling, J.E. Ffowcs Williams, M. Heckl, F.G. Leppington, in: Modern Methods in Analytical Acoustics (Lecture Notes), Springer, London, 1992.
[23] T. Kambe, T. Minota, Sound radiation from vortex systems, *Journal of Sound and Vibration* 74 (1981) 61–72.
[24] T. Kambe, T. Minota, Acoustic wave radiated by head-on collision of two vortex rings, *Proceedings of the Royal Society of London A* 386 (1983) 277–308.
[25] S.K. Tang, N.W.M. Ko, Sound generation by a vortex ring collision, *Journal of the Acoustical Society of America* 98 (1995) 3418–3427.
[26] Y. Nakashima, Sound generation by head-on and oblique collisions of two vortex rings, *Physics of Fluids* 20 (2008) 056102.
[27] Y. Nakashima, O. Inoue, Sound generation by a vortex ring collision with a wall, *Physics of Fluids* 20 (2008) 126104.